Clinicopathologic significance of nuclear HER4 and phospho-YAP(S^{127}) in human breast cancers and matching brain metastases

Priyakshi Kalita–de Croft iD **, Malcolm Lim, Haarika Chittoory** iD **, Xavier M. de Luca, Jamie R. Kutasovic, Bryan W. Day, Fares Al-Ejeh** iD **, Peter T. Simpson, Amy E. McCart Reed, Sunil R. Lakhani* and Jodi M. Saunus***

Abstract

Background: Human epidermal growth factor receptor-4 (HER4) and yes-associated protein-1 (YAP) are candidate therapeutic targets in oncology. YAP's transcriptional coactivation function is modulated by the HER4 intracellular domain (HER4-ICD) *in vitro*, but the clinical relevance of this has not been established. This study investigated the potential for targeting the HER4-YAP pathway in brain metastatic breast cancer.

Methods: We performed immuno-phenotypic profiling of pathway markers in a consecutive breast cancer series with 25 years of clinical follow up ($n = 371$), and patient-matched breast and metastatic brain tumours ($n = 91$; 30 pairs).

Results: Membrane localisation of phospho-HER4 [pHER4(Y^{1162})] was infrequent in primary breast cancer, but very frequent in brain metastases (5.9% *versus* 75% positive), where it was usually co-expressed with pHER3(Y^{1289}) ($p < 0.05$). The presence of YAP in tumour cell nuclei was associated directly with nuclear pERK5(T^{218}/Y^{210}) ($p = 0.003$). However, relationships with disease-specific survival depended on oestrogen receptor (ER) status. Nuclear pYAP(S^{127}) was associated with smaller, good prognostic ER+ breast tumours (log-rank hazard-ratio 0.53; $p = 9.6E^{-03}$), but larger, poor prognostic triple-negative cancers (log-rank hazard-ratio 2.78; $p = 1.7E^{-02}$), particularly when co-expressed with nuclear HER4-ICD ($p = 0.02$). This phenotype was associated with stemness and mitotic instability markers (vimentin, SOX9, ID1, SPAG5, TTK, geminin; $p < 0.05$). YAP expression in brain metastases was higher than matched primary tumours; specifically, nuclear pYAP(S^{127}) in ER-negative cases ($p < 0.05$). Nuclear YAP was detected in ~70% of ER-negative, HER4-activated brain metastases.

Discussion: Our findings suggest that the canonical-mechanism where Hippo pathway-mediated phosphorylation of YAP ostensibly excludes it from the nucleus is dysfunctional in breast cancer. The data are consistent with pYAP(S^{127}) having independent transcriptional functions, which may include transducing neuregulin signals in brain metastases. Consistent with mechanistic studies implicating it as an ER co-factor, nuclear pYAP(S^{127}) associations with breast cancer clinical outcomes were dependent on ER status.

Conclusion: Preclinical studies investigating HER4 and nuclear YAP combination therapy strategies are warranted.

Keywords: brain metastasis, breast cancer, biomarkers, HER4

Correspondence to:
Priyakshi Kalita–de Croft
The University of Queensland Faculty of Medicine, UQ Centre for Clinical Research, Building 71/98 Royal Brisbane and Women's Hospital, Herston, Qld 4006, Australia
p.kalita@uq.edu.au

**Malcolm Lim
Haarika Chittoory
Xavier M. de Luca
Jamie R. Kutasovic
Peter T. Simpson
Amy E. McCart Reed
Jodi M. Saunus**
The University of Queensland Faculty of Medicine, UQ Centre for Clinical Research, Herston, Qld, Australia

Bryan W. Day
QIMR Berghofer Medical Research Institute, Herston, Qld, Australia

Fares Al-Ejeh
QIMR Berghofer Medical Research Institute, Herston, Qld, Australia

Permanent address: Qatar Biomedical Research Institute (QBRI), Hamad Bin Khalifa University, Qatar Foundation, Doha

Sunil R. Lakhani
The University of Queensland Faculty of Medicine, UQ Centre for Clinical Research, Herston, Qld, Australia

Pathology Queensland, The Royal Brisbane and Women's Hospital Herston, Qld, Australia

*These authors contributed equally.

Introduction

Relapse of breast cancer in the brain leads to significant morbidity and premature death, generally within 2 years of diagnosis.[1] Epidemiological data indicate that symptomatic brain metastases are diagnosed in approximately 15% of metastatic breast cancer patients,[2] but develop in as many as 40% with disseminated disease.[1,3–5] Patients with HER2-positive (HER2+) and triple-negative breast cancer (TNBC) are more likely to develop brain metastases than those with oestrogen receptor-positive (ER+) breast cancer,[6,7] indicating there are subtype-specific determinants of metastasis to the brain. Treatment can include surgical resection, focused or whole-brain radiotherapy and chemotherapy.[8] These interventions can improve quality-of-life and overall life expectancy but are rarely curative. Together with population ageing, better systemic cancer control and prolonged patient survival are likely to further elevate the incidence of brain-metastatic breast cancer in the future.[9,10]

There is a shortage of molecular-targeted therapeutics for effective treatment of brain metastases. Resolving this requires a deeper understanding of their vulnerabilities. One approach is to identify molecular features that set them apart from their parent primary cancers, which potentially represent brain-specific adaptations required for outgrowth. Another is to identify targetable molecular alterations that are frequent in brain metastases regardless of their status in the primary tumour, which may be more broadly applicable and amenable to drug repurposing. Analysis of patient-matched primary and metastatic tumours has been applied to identify candidates in both categories.[11–14] For example, we and others showed that human epidermal growth factor receptors (HER) are pivotal to brain metastasis pathogenesis; particularly HER2 and HER3.[11,13,15,16] These receptors promote tumour progression through ligand-dependent activation. Abundant in the brain,[17] neuregulin growth factors bind to HER3, resulting in dimerization, cross-phosphorylation and recruitment of relay proteins that bring about oncogenic cellular changes, notably including potent activation of PI3K.[18,19] HER3 induction is one of many adaptations that occur as metastatic cells opportunistically exploit the brain microenvironment.[20–23]

HER4 is also responsive to neuregulins, can dimerise with other HERs and is frequently activated in brain metastases.[16,24] There are currently no specific inhibitors of HER4, but several agents with pan-HER activity are under clinical development, including neratinib, afatinib, dacomitinib and poziotinib. Clinical evidence that HER4 activity could be an important mediator of brain metastasis came from the randomised phase III NALA trial, which compared lapatinib (standard-of-care inhibitor of EGFR and HER2) with neratinib (inhibitor of EGFR, HER2 and HER4), both in combination with capecitabine, for treatment of HER2+ metastatic breast cancer.[25] The neratinib regimen doubled 12-month progression-free survival (PFS) and significantly delayed the time to intervention for symptomatic intracranial disease. Based on these findings, the United States Food and Drug Administration (FDA) approved neratinib for patients with treatment-refractory, metastatic HER2+ breast cancer.[26] The potential for delaying intracranial disease in clinically HER2-negative breast cancer has not yet been established.

Apart from canonical receptor tyrosine kinase (RTK) activity, ligand-activated HER4 also undergoes juxta- and intra-membrane proteolysis, releasing a C-terminal intracellular domain (HER4-ICD) that can translocate to the nucleus. In the mammary gland, HER4-ICD transcriptional coactivation of STAT5A is essential for normal lobuloalveolar development, epithelial differentiation and milk production.[27,28] In breast cancer, it is reportedly an ER cofactor associated with poor prognosis in ER+ disease,[29] but results have been mixed, with a literature meta-analysis finding no overall relationship with survival.[30] A direct interaction between HER4-ICD and the oncogenic transcription coactivator, YAP (yes-associated protein), has been identified in breast tumour cell line nuclei: HER4-ICD directly induced YAP-regulated genes and pro-metastatic cell behaviour *in vitro*,[31,32] but the clinical relevance of this interaction has not been established.

Recently implicated in brain metastatic outgrowth in a mouse model of metastatic lung cancer as well as in human lung-brain metastasis,[33,34] YAP is a transcriptional coactivator of the TEAD family of transcription factors. Collectively they regulate proliferation, cell fate and survival, with a large body of evidence now pointing to a role in microenvironment recognition.[35,36] YAP-TEAD complexes are opposed by the Salvador-Warts-Hippo ('Hippo') pathway, which serves the evolutionarily conserved purpose of maintaining equilibrium according to tissue growth and cellular density cues. Hippo pathway kinases

Table 1. Cohort characteristics.

Key demographics	General BC cohort	Brain-metastatic BC cohort	
Median age at BC dx	59.3 years	49 years	
Median age at BrM dx	NA	52 years	
Disease-specific survival (median years)	13.9 (overall follow-up) 4.83 (censored deaths)	0.92 (after BrM dx)	
Molecular subtypes (% of evaluable cases)	BC	Br.MBC	BrM
ER+/HER2-	76%	23%	20%
HER2+	12%	34%	35%
TNBC	17%	42%	43%
Total samples (*n*)	371	41*	50*

*Of informative TMA samples this represents 30 matched pairs.
BC, breast cancer; BrM, brain metastases; br.MBC, brain metastatic breast cancers; ER, oestrogen receptor; HER, human epidermal growth factor receptor; NA, not applicable.

LATS1/2 phosphorylate YAP on five conserved HXRXXS motifs, including one at serine-127 [pYAP(S^{127})] that mechanistic studies indicate is necessary for 14-3-3 binding and cytosolic retention, ultimately leading to proteolysis.[37] YAP and its close paralog TAZ are dysregulated in a variety of cancers, with disconnection from Hippo pathway control critical for bypassing normal growth constraints.[36,38] Secondary onco-protective actions of several agents used to treat congestive heart failure and inflammation may be partly mediated by impairing nuclear translocation of YAP (e.g. dasatinib, statins, pazopanib and several others directly modulate YAP's interaction with its primary TEAD transcription factors [e.g. digitoxin and the COX-inhibitor, flufenamic acid)].

Functional and histopathology studies mostly concur that YAP expression is oncogenic, and that its activity in the nucleus plays a major role in mediating resistance to a number of different molecular-targeted agents.[39–43] But paradoxically, YAP expression is reportedly a favourable prognostic indicator in oestrogen receptor-positive (ER+) breast cancers.[41,44] Also still to be resolved is the observation that the phosphorylated YAP isoform typically associated with cytosolic retention [pYAP(S^{127})] has been detected in tumour cell nuclei of both primary and metastatic breast tumours, including brain metastases.[40,45]

The aim of this study was therefore to analyse the expression and phosphorylation status of HER4 and YAP in human breast cancer samples, with a view to developing a better understanding of their potential as therapeutic targets in early and/or metastatic breast cancer. From a biological point of view, we also wanted to explore the idea that expression and activation of HER4 are linked to YAP activation in brain metastases.

Methods

This study involved immunohistochemistry (IHC) analysis of: (1) a clinically annotated, consecutive series of primary breast tumours with >20 years follow up, herein referred to as the 'general breast cancer cohort' (described previously)[46–52]; and (2) patient-matched pairs of primary and brain-metastatic breast tumours, herein referred to as the 'brain-metastatic breast cancer cohort' (br.MBC) (Table 1). Both were sourced from the same diagnostic pathology centres in Queensland, Australia, and represent a similar patient population. Ethical approval for this study was obtained from human research ethics committees of the Royal Brisbane and Women's Hospital (RBWH; 2005000785) and The University of Queensland (HREC/2005/022). Written consent to use tissue specimens and de-identified clinical data for research purposes is not a requirement under these approvals because the samples were

Table 2. Biomarkers analysed by IHC.

Target	Scoring criteria
HER4	Cytoplasmic intensity: negative/low or moderate/strong Nuclear positive if any staining detected
pHER4(Y^{1162})	Cytoplasmic intensity: negative or positive Membrane-positive if continuous staining in $\geq$10% tumour cells
YAP	Cytoplasmic intensity: negative/low or moderate/strong Nuclear positive if any staining detected
pYAP(S^{127})	Cytoplasmic intensity: negative or positive Membrane-positive if continuous staining in $\geq$10% tumour cells
pEGFR(Y^{1068})	Membrane-positive if continuous staining in $\geq$10% tumour cells
pHER2($Y^{1221/1222}$)	Membrane-positive if continuous staining in $\geq$10% tumour cells
pHER3(Y^{1289})	Membrane-positive if continuous staining in $\geq$10% tumour cells
pERK5(T^{218}/Y^{210})	Nuclear positive if any staining detected
ID1	Nuclear positive if any staining detected
SPAG5	Negative or positive (cut-off used: h-score $\geq$100)
SOX9	Nuclear positive if any staining detected

EGFR, epidermal growth factor receptor; HER, human epidermal growth factor receptor; IHC, immunohistochemistry; YAP, yes-associated protein-1.

sourced from pathology archives of the 1980s, and most patients are now deceased. Samples were de-identified for all the analyses performed in this study.

Tumours were sampled in tissue microarrays (TMAs) for IHC analysis of proteins in the HER4-YAP pathway, and other biomarkers of interest (Table 2). Maximum scores of duplicate cores were used for analysis.

Tumour tissue cohorts, histopathology and clinico-pathologic characterisation

A breast cancer-brain metastasis resource cohort was assembled from formalin-fixed paraffin-embedded (FFPE) primary breast cancer and patient-matched BrM samples of patients who had treatment in Queensland, Australia, between 2000 and 2018. Cases were identified on the basis of BrM tissue availability, then filtered based on availability of corresponding primary breast tumour tissue. Clinical diagnostic information and survival data were obtained from Pathology Queensland, Queensland Health and the Queensland Cancer Registry. Tumours were

sampled in TMAs for IHC analysis (1 mm cores), with hematoxylin and eosin staining used to locate the tumour component of surgical specimens. A comprehensive histopathological review of all cases was conducted by experienced molecular pathologists (SRL, JMS). Clinico-pathologic information (e.g. histological type, grade and stage) and survival data were assembled in a database linked by the TMA position of each case. We assessed clinical biomarkers by IHC (see in the following) according to diagnostic reporting standards, as described previously[46]: (i) oestrogen and progesterone receptors (hormone receptors, HR); (ii) human epidermal growth factor receptor 2 (HER2).

Immunohistochemistry

IHC antibodies and staining conditions are detailed in Table 3. Primary antibodies were selected on basis of prior use in published reports (preferably for IHC applications) and a manufacturer specificity guarantee. Before applying the antibodies to test sample cohorts, we also validated their specificity experimentally, first by confirming substantially reduced IHC signal in cell lines depleted of their

Table 3. Antibodies and conditions used for IHC analysis.

Target	Manufacturer	Clone	Host	Antigen retrieval	Dilution	Incubation
HER4	Santa Cruz	C-18	Rabbit	EDTA-pH 8.8	1/2500	Overnight
pHER4(Y^{1162})	Abcam	EP2270Y	Rabbit	EDTA pH 8.8	1/100	Overnight
pEGFR (Y^{1068})	Cell signaling	D7A5	Rabbit	EDTA pH 8.8	1/25	1 h
pHER2(Y$^{1221/1222}$)	Cell signaling	6B12	Rabbit	EDTA pH 8.8	1/200	1 h
pHER3 (Y^{1289})	Cell signaling	21D3	Rabbit	EDTA pH 8.8	1/50	1 h
YAP	Cell signaling	D8H1X	Rabbit	Citrate pH 6.0	1/100	Overnight
pYAP(S^{127})	Cell signaling	poly	Rabbit	Citrate pH 6.0	1/250	Overnight
pERK5(T^{218}/Y^{210})	Cell signaling	poly	Rabbit	Citrate pH 6.0	1/175	Overnight
ID1	Santa Cruz Biotech.	sc-133104	Mouse	EDTA pH 8.8	1/100	Overnight
SPAG5	Sigma Aldrich	Poly	Rabbit	Citrate pH 6.0	1/50	Overnight
SOX9	Merck Millipore	Poly	Rabbit	Citrate pH 6.0	1/5000	Overnight

EGFR, epidermal growth factor receptor; HER, human epidermal growth factor receptor; IHC, immunohistochemistry; YAP, yes-associated protein-1.

targets by siRNA (section *siRNA-mediated depletion of IHC antibody targets and antibody validation studies*, Supplemental Figure S1A/B); and second, by reviewing a range of normal human tissue types stained using the intended IHC protocol, cross-referencing the literature and Human Protein Atlas.[53] Finally, IHC conditions were specifically optimised for the test samples, which are several decades old and often require different antigen retrieval conditions compared with cell line pellets or newer tissue samples.

IHC was performed on 4 μm FFPE TMA sections using the Mach1 Universal HRP-Polymer Detection Kit (BioCare Medical, Pacheco, CA, USA). Briefly, sections were deparaffinized with xylene and hydrated in a graded ethanol series (95–70%). Heat-induced antigen retrieval was performed using a decloaking chamber (BioCare Medical) with sodium citrate buffer (0.01 M, pH 6.0) for 5 min at 125°C, or EDTA buffer (0.001 M, pH 8.8) for 30 min at 95°C. Antigen retrieval was performed using α-chymotrypsin (Sigma-Aldrich, St. Louis, MO, USA) for 10 min at 37°C. Sections were rinsed with tris-buffered saline (TBS), then treated with 0.3% hydrogen peroxide for 10 min. Non-specific staining was blocked with MACH1 Sniper blocking reagent (BioCare Medical). Primary antibody in TBS was applied to the slide for 1 h at room temperature or overnight at 4°C in a humidified slide chamber. For rabbit primary antibodies, MACH1 anti-rabbit secondary antibody conjugated to horseradish peroxidase was applied for 30 min at room temperature. Diaminobenzidine chromogen substrate was applied for 1–5 min. Lastly, slides were counterstained with hematoxylin for 30 s and cover-slipped with DPX mountant (Sigma-Aldrich). For analysis, stained slides were scanned at 40× magnification using an Aperio AT Turbo (Leica Biosystems, Wetzlar, Germany).

IHC scoring and analysis
High resolution digital IHC light microscopic images were used to assess IHC staining. Scoring of the tumour compartment of TMA cores was performed by at least two independent observers, according to criteria determined during a combined preliminary review. Individual TMA core images were linked to a database containing other clinicopathologic data by a TMA position code, then reviewed in a blinded manner. Statistical testing was done using GraphPad PRISM Software (v8.2; GraphPad Software, San Diego, CA, USA), with specific tests indicated accordingly in the main text and figure legends. p values <0.05 were considered significant.

siRNA-mediated depletion of IHC antibody targets and antibody validation studies

Cell lines (T47D and MDA-MB-468) were purchased from the American Type Culture Collection (Manassas, VA, USA), maintained in recommended culture conditions and regularly screened for Mycoplasma. For transient knockdown studies, cells were transfected with 100 nM siRNAs comprising of a mixture of three different sequences for each gene (Gene Pharma, Shanghai, China) using FugeneHD (Promega, Madison, WI, USA): YAP-homo-1858, CUGCCACCAA GCUAGAUAATT; YAP-homo-1517, GACGA CCAAUAGCUCAGAUTT; YAP-homo-862, GCAUCUUCGACAGUCUUCUTT; ERBB4-homo-1815, GGUCCUGACAACUGUACA ATT; ERBB4-homo-2474, CCAGCUGGUU ACUCAACUUTT; ERBB4-homo-3213, ACU GAGCUCUCUCUCUGACTT; negative control, UUCUCCGAACGUGUCACGUTT. After 24 h, cells were fixed in 10% neutral buffered formalin (Sigma) and paraffin embedded. Cell pellet sections (6 μm) were heat-retrieved in antigen retrieval buffers as indicated in Table 3 using a Decloaking Chamber in Background Sniper blocking solution (Biocare Medical). Slides were incubated with primary antibodies as indicated in Table 3. Detection was performed using the Mach1 kit (Biocare Medical). Slides were then scanned and imaged on an Aperio AT Turbo slide scanner (Leica Biosystems).

Datasets and statistics

The following datasets were analysed in this study: TCGA breast cancer RNASeq (V2 RSEM) dataset (mRNA expression z-scores); GISTIC 2.0 putative copy-number calls (provisional TCGA breast tumour dataset)[54]; and METABRIC invasive breast cancer dataset (mutation calls, accessed *via* cBioPortal).[55] TCGA breast cancer clinical data was linked from the pan-cancer clinical data resource (CDR).[56] Preparation of graphs and statistical analyses were performed using GraphPad Prism software (v8.2). Unless specific p-values are indicated: $\star p = 0.05{-}0.01$; $\star\star p < 0.01$.

Results

Expression and activation of HER4 in major breast cancer subtypes

We used a HER4 antibody that recognises a C-terminal epitope in all known isoforms to perform IHC analysis in the general breast cancer series. This antibody was validated for specificity using siRNA mediated gene knockdown (Supplemental Figure S1A). In line with published data,[57–59] we considered nuclear staining to represent nuclear HER4-ICD, and cytoplasmic staining as a mixture of isoforms, including mitochondrial HER4-ICD and a range of trafficking intermediates. IHC analysis revealed expression of HER4 in tumour cell nuclei as well as cytoplasm (Figure 1A) and approximately half of all cases were positive (Supplemental Table S1). There was a direct relationship between nuclear and cytoplasmic expression, particularly in TNBC (Figure 1B; $p = 1.1E^{-07}$), indicating that in most breast tumours within this cohort, HER4 is either absent or present in both compartments at the same time. However, there were exceptions that presented an opportunity to investigate compartment-specific biology. Amongst HER4+ cases, we considered that nuclear-predominant (no/low cytoplasmic HER4) and cytoplasmic-predominant (no nuclear HER4-ICD) may exemplify distinct biology. There were no differences in these patterns between ER+, HER2+ and TNBC cases (Figure 1C). Nuclear-4ICD was weakly associated with shorter survival, though these differences were not statistically significant (Figure 1D).

Phospho-HER4 (pHER4) functions at the plasma membrane and has separate functions to HER4-ICD. We performed IHC analysis of the general breast cancer cohort using an antibody against phospho-tyrosine 1162 [pHER4(Y^{1162})]. Tumour cell membrane staining was detected in 5.9% of cases ($n = 16/371$). Membranes were stained strongly and continuously, and regions with compact architecture tended to express pHER4(Y^{1162}) at the edges (Figure 1E). This spatial heterogeneity is consistent with receptor activation requiring access to stromal ligands. We also assessed Ki67, EGFR, CK14 and CK5/6 as surrogate markers of breast cancer molecular subtypes,[46] and confirmed that membrane-pHER4 positivity is associated with HER2+ breast cancer (Figure 1Fi; $p = 2.0E^{-05}$). Amongst HER2+ cases, membrane-pHER4 positivity was associated directly with Ki67 expression (Figure 1Fii; $p = 0.03$), suggesting a relationship with proliferation in HER2-amplified tumours. There was no association with survival (Figure 1G), but it should be noted that this archival cohort pre-dates the introduction of Herceptin in Australia.
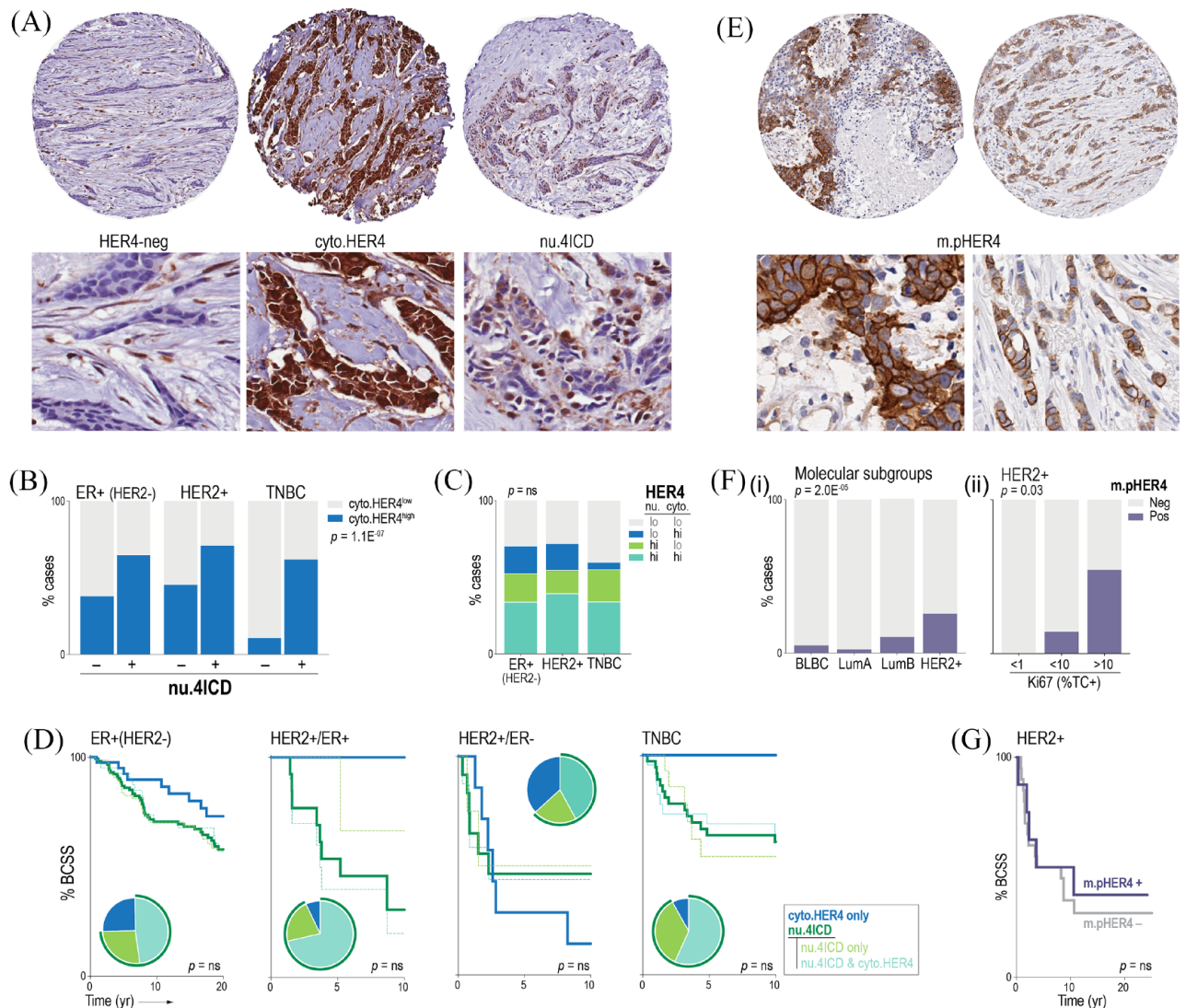
Figure 1. Expression and activation of HER4 in early breast cancer. (A) Representative breast tumour cores stained for HER4. (B) Chi-square analysis of the proportions of nuclear and cytoplasmic HER4 staining in major breast cancer subtypes. (C) Chi-square analysis of the proportions of cases exhibiting compartment specific HER4 staining. (D) KM analysis of the relationships between HER4 compartment categories (blue and green) and BCSS. Pie charts indicate proportion of cohort in each category. (E) Representative tumour cores stained for pHER4(Y[1162]). (F) Chi-square analysis of the proportions of cases with pHER4(M+) across molecular subtypes (i) and proliferative status of HER2+ cases (ii). (G) Kaplan–Meier analysis of relationships between pHER4(M) staining and BCSS.

BCSS, breast cancer-specific survival; BLBC, basal-like breast cancer; HER4, human epidermal growth factor receptor-4; LumA/B, luminal A/B; Ki67 %TC+, percentage of tumour cells positive for proliferation marker Ki67; KM, Kaplan–Meier; pHER4(M+), pHER4 membrane positivity.

HER4 is induced and activated in breast cancer brain metastases

We next analysed HER4 and pHER4 in patient-matched primary breast cancers and brain metastases. Compared with the general breast cancer cohort, where the incidence of brain metastases is estimated to be 5–10%,[2,60] there were no significant differences in HER4 or pHER4 in brain metastatic breast cancers (Figure 2A; BC *versus* br.MBC). However, brain metastases exhibited

clear induction and activation of HER4 in 75% of cases (Figure 2A; BC/br.MBC *versus* BrM). Paired analyses highlighted that this phenotype is particularly prominent in HER2+ and TNBC cases (Figure 2B; 4.0E[−06]). In order to investigate whether this was associated with other HER family members, we also analysed levels of membrane-associated expression of HER4's dimerization partners pEGFR, pHER2 and pHER3. Most primary breast tumours exhibited very low
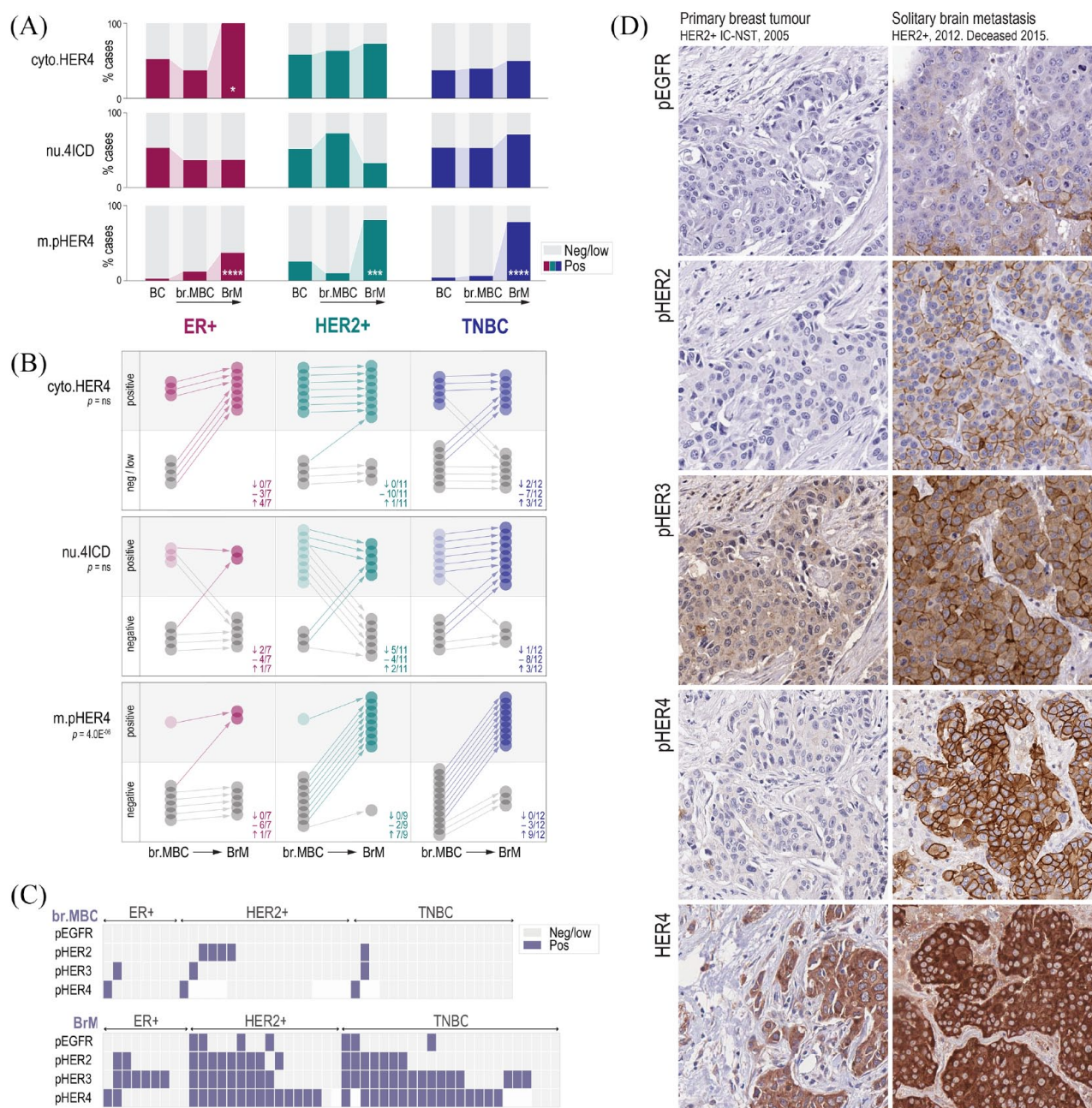
Figure 2. Expression and activation of HER4 in brain-metastatic breast cancers and brain metastases. (A) Chi-square analysis of cyto.HER4, nu.4ICD and m.pHER4 in major breast cancer subtypes. $*p < 0.05$; $***p < 0.001$; $****p < 0.0001$. (B) Changes in cyto.HER4, nu.4ICD and m.pHER4 in individual matched cases, separated according to major breast cancer subtypes. Chi-square p-values indicate significant differences before and after metastasis to the brain. (C) Tile plot showing overall numbers of br.MBC and BrM co-expressing pHER receptors (columns are individual tumours). (D) Representative IHC analysis of samples from a patient whose HER2+ breast cancer recurred in the brain 7 years after diagnosis and treatment with HER2-targeted therapy. This case exemplifies concomitant induction of pHER2, pHER3 and pHER4.

BrM, brain metastases; br.MBC, brain metastatic breast cancers; cyto.HER4, cytoplasmic HER4; HER4, human epidermal growth factor receptor-4; IC-NST, invasive carcinoma, no special type; IHC, immunohistochemistry; LumA/B, luminal A/B; m.pHER4, membrane-pHER4; nu.4ICD, nuclear HER4-ICD.

levels of activated HER isoforms, but there was substantial induction of membrane-associated pHER3 concomitant with pHER4 (Figure 2C/D; $p < 0.05$) in brain metastases. Altogether, 69% of pHER4+ brain metastases also expressed pHER3 (Figure 2C). Taken together, these findings suggest

that tumour cell HER3 and HER4 transduce exogenous neuregulin growth signals from the brain tumour microenvironment.

Nuclear pYAP(S127) is an ER-dependent prognostic indicator in breast cancer

Previous studies have demonstrated that nucleo-cytoplasmic shuttling and phosphorylation are important modulators of YAP's transcriptional activity,[35,36,61] but the clinical relevance in breast cancer has not been clearly established. We analysed the expression of YAP and pYAP(S^{127}) in the general breast cancer cohort using validated IHC antibodies (Supplemental Figure S1B). Staining was homogeneous in breast tumour cell cytoplasm and/or nuclei (Figure 3A), and neither YAP nor pYAP(S^{127}) was associated with histological type, grade, HER2 or ER status (Supplemental Tables S2 and S3). There was a direct association between nuclear and cytoplasmic YAP (Figure 3Bi; $p < 1.0E^{-06}$), and the cytoplasmic pool was phosphorylated in the majority of cases (average 74%; Figure 3Bii; $p < 1.0E^{-06}$). But this was also the case for the nuclear compartment, with YAP phosphorylation evident in 66% of nuclear YAP[high] cases overall (Figure 3Biii; $p < 1.0E^{-06}$). Conversely, around one-third of cases with low cytoplasmic pYAP(S^{127}) exhibited strong nuclear pYAP(S^{127}) (Figure 3Biv; $p < 1.0E^{-06}$).

We explored the clinical significance of pYAP(S^{127}) being localised to tumour cell cytoplasm or nuclei by performing Kaplan–Meier analysis. Cytoplasmic pYAP(S^{127}) was generally protective in this cohort, but phosphorylation of the nuclear pool stratified survival oppositely depending on ER status (Figure 3C). Strikingly, nuclear pYAP(S^{127}) was a favourable prognostic indicator in ER+ cases but marked poor prognosis in TNBC (Figure 3C). In the ER+ cases (Figure 3Ciii) the hazard-ratio associated with nuclear pYAP(S^{127}) was 0.53 (log-rank test; 95% CI: 0.35–0.81; $p = 9.6E^{-03}$) whereas, in TNBC the hazard-ratio associated with was 2.78 (Figure 3Civ) (log-rank test; 95% CI: 1.31–5.92; $p = 1.7E^{-02}$). To account for the fact that pYAP(S^{127}) is often present in cytoplasmic and nuclear compartments at the same time (Figure 3Biv), we performed the analysis after categorising cases into subgroups with: (1) negative/low pYAP expression (light grey); (2) cytoplasm-predominant pYAP(S^{127}) (cyto>>nucleus; orange); (3) nuclear-predominant pYAP(S^{127}) (nucleus>>cyto; purple); or (4) high levels of pYAP(S^{127}) in both compartments, (uniformly high; dark grey) (Figure 3Cv/vi). The results were consistent, with pYAP(S^{127}) associated with good prognosis in ER+ cases (Figure 3Cv; $p = 7.5E^{-04}$) regardless of localisation, but poor prognosis when present in nuclei of ER-negative breast cancer (Figure 3Cvi; $p = 2.0E^{-02}$).

Others have reported that *YAP1* is a target of 11q22 amplification in a range of human cancer types, and that this can underpin over-expression and correspondingly higher levels of serine-127 phosphorylation in cell lines.[62] We therefore investigated the frequency of *YAP1* copy-number alterations (CNAs) to see whether this could be related to the pYAP(S^{127}) phenotype. Analysis of TCGA breast cancer RNAseq and CNA datasets showed there is a direct relationship between *YAP1* copy number and RNA expression (Figure 3Di; $p < 1.0E^{-15}$), with significantly more *YAP1* gain or amplification in TNBCs (Figure 3Dii; $p = 8.6E^{-11}$). There was a modest difference in TNBC-specific survival amongst cases with *YAP1* gain *versus* loss in TNBCs (Figure 3Diii; $p = 0.07$), though this did not approach the degree of stratification associated with protein level expression, phosphorylation and subcellular localisation.

Nuclear pYAP(S127) has ER-dependent relationships with breast tumour size, ERK5 and HER4

Since YAP promotes the phosphorylation and nuclear translocation of ERK5 in myogenesis,[63] we performed IHC analysis of nuclear pERK5 as candidate marker of YAP activity in breast cancer. There were no marked changes in the frequency of unphosphorylated YAP expression according to nuclear pERK5 status, but pYAP(S^{127}), particularly the nuclear pool, was directly associated with nuclear pERK5 (Figure 4A). The working model of YAP function denotes that LATS-mediated phosphorylation at serine-127 *limits* its activity, reflecting Hippo pathway-mediated negative feedback on growth,[64,65] and yet this result, together with the analysis of breast cancer-specific survival (Figure 3), suggest that nuclear pYAP(S^{127}) might be an active isoform in breast cancer.

In normal tissues, hippo pathway-mediated phosphorylation and cytoplasmic sequestration of YAP limit tissue growth. We found associations between nuclear pYAP(S^{127}) and breast tumour size that were consistent with survival data, with nuclear pYAP(S^{127}) inversely associated with ER+ tumour size, but directly associated with ER-negative
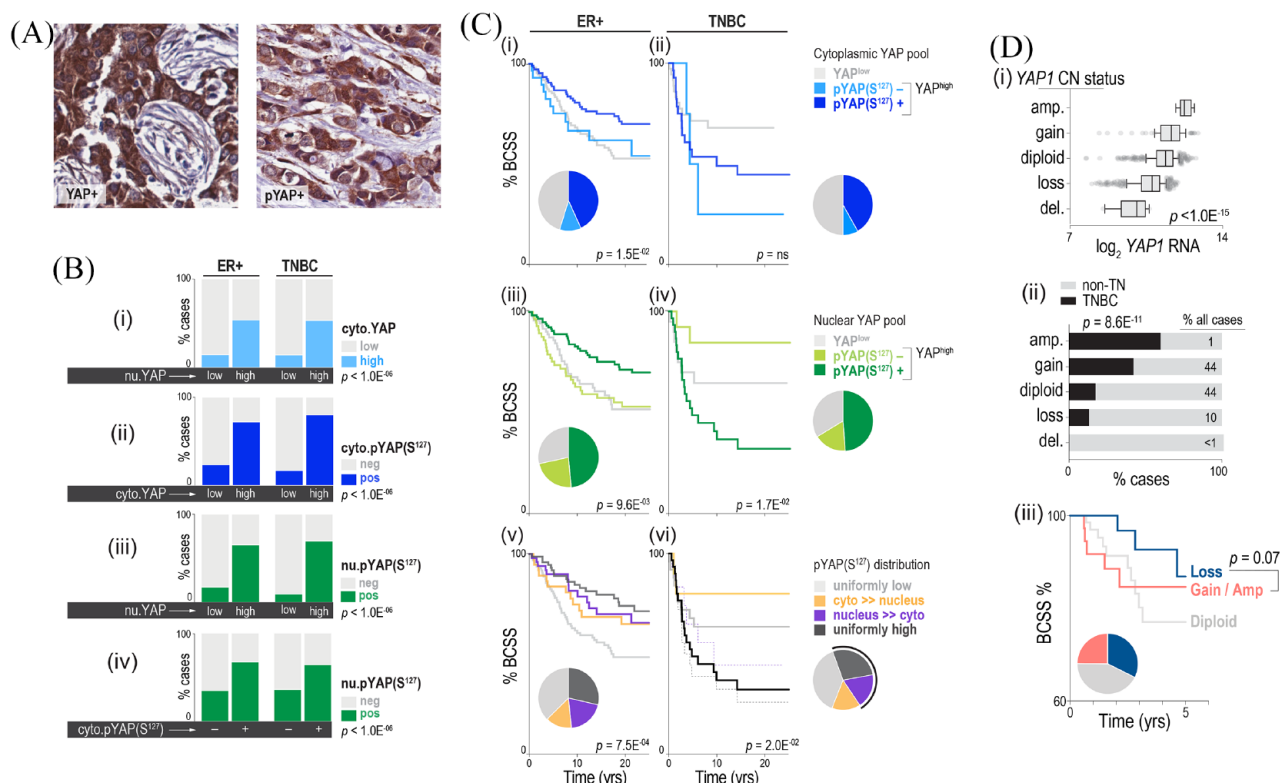
Figure 3. Expression and activation of YAP in early breast cancer, and relationship with patient survival.
(A) Representative images of breast cancer cores stained with antibodies specific for YAP and pYAP(S^{127}). (B) Contingency analysis in ER+ and TNBCs showing: (i) cyto.YAP intensity relative to nu.YAP intensity; (ii) cyto.pYAP(S^{127}) status relative to total cyto.YAP; (iii/iv) nu.pYAP(S^{127}) status relative to overall nuclear YAP levels or cyto.pYAP(S^{127}). Chi-square *p*-values shown. (C) KM analysis of relationships between YAP phosphorylation and BCSS in ER+ (left panel) and TNBC (right panel) cases. Analyses were designed to examine the effect of phosphorylation of the cytoplasmic or nuclear protein pools, and the relationships between pYAP(S^{127}) subcellular distribution and BCSS. Pie charts show relative proportions of cases in each category. Statistical significance determined using log rank tests. TNBC subgroups 'nucleus>>cyto' and 'uniformly high' were combined for statistical testing (bottom right). (D) (i) Relationship between *YAP1* gene copy number and RNA expression. Kruskal–Wallis *p*-value shown. (ii) Proportions of TN and non-TN TCGA breast cancers with copy-number alterations. Chi-square *p*-value shown. (iii) KM analysis comparing survival of TNBCs (TCGA) with loss *versus* gain/amplification (amp) of the *YAP1* gene.
BCSS, breast cancer-specific survival; cyto.YAP, cytoplasmic YAP; ER+, oestrogen receptor positive; KM, Kaplan–Meier; nu.YAP, nuclear YAP; TCGA, The Cancer Genome Atlas; TN, triple negative; TNBC, triple negative breast cancer; YAP, yes-associated protein-1.

tumour size. Subcellular distribution analysis confirmed that not only is the phosphorylated isoform more frequent overall, but pYAP(S^{127}) is preferentially localised to the nucleus in larger ER-negative tumours (Figure 4B).

As YAP activity is regulated by HER4-ICD *in vitro*,[32,66] we next looked for relationships between these proteins in the breast tumour cohort. Nuclear pYAP(S^{127}) was slightly more frequent in HER4-ICD+ ER+ tumours but, overall, nuclear pYAP(S^{127}) and HER4-ICD phenotypes were largely independent (Figure 4C). In contrast, their co-expression did have an effect in survival analysis, stratifying survival to a greater degree than the status of nuclear pYAP(S^{127}) alone, particularly in TNBC and particularly within the first 10 years of diagnosis (Figure 4D).

YAP activity has been linked to stem cell attributes in a range of cancers, including chromosomal instability, E-cadherin loss, mesenchymal features and the induction of *SOX9*.[36,39,40,67–69] Consistent with this, meta-analysis of previously published data from this cohort[49,70,71] showed there are direct associations between pYAP(S^{127}) and basal cytokeratins, the mesenchymal marker vimentin, stem cell factors (SOX9, ID1), and markers of chromosomal and mitotic instability (SPAG5, TTK, geminin) (Figure 4E).

Taken together, these data suggest that ER is a key determinant of YAP function, that nuclear pYAP(S^{127}) may be an active isoform in TNBC and that the previously identified transcriptional interaction with nuclear HER4-ICD[32,66] could be relevant in human disease.
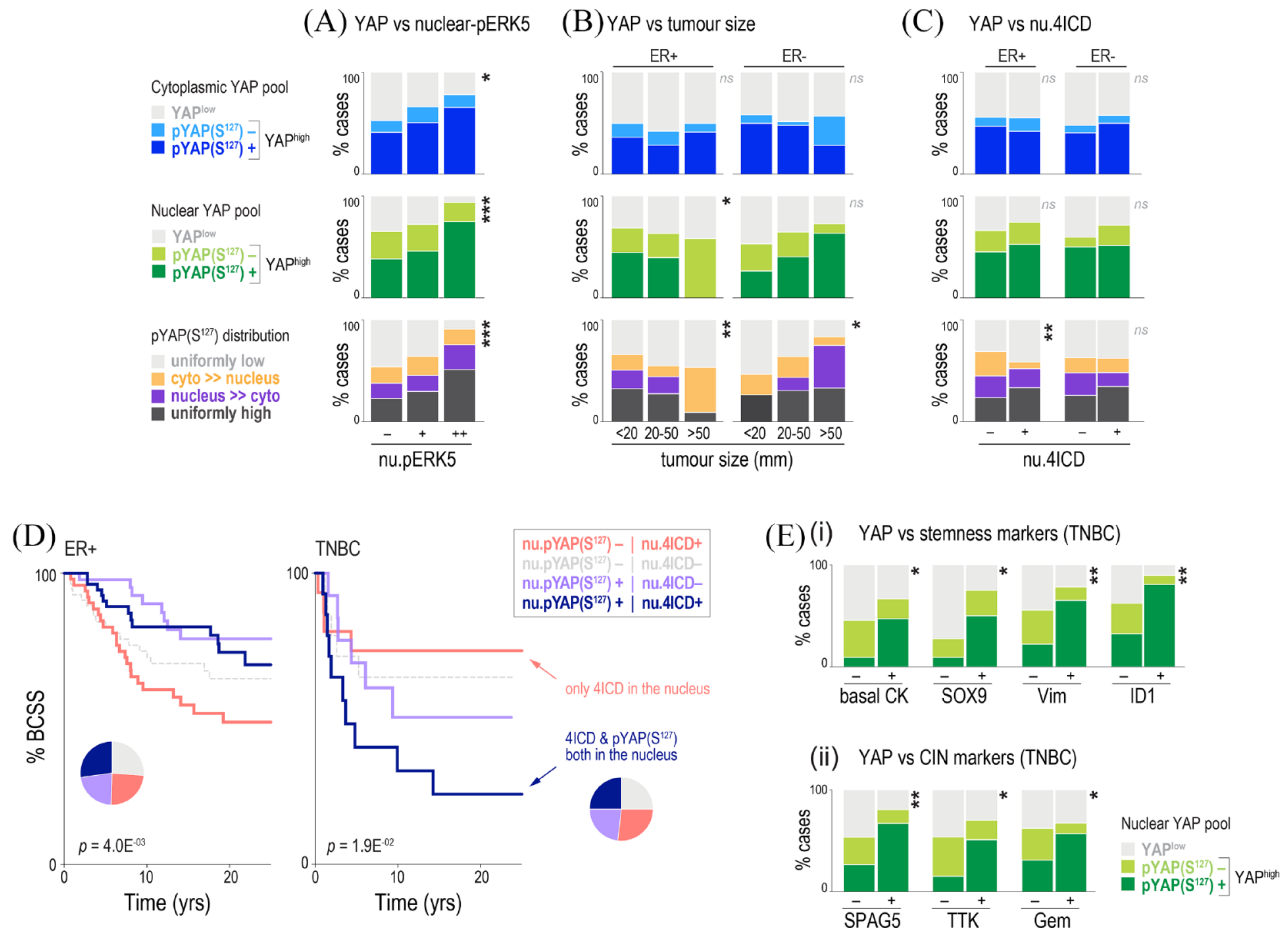
**Figure 4.** Clinico-pathologic correlates of cytoplasmic- or nuclear-localised pYAP(S127).
Bar graphs show YAP phosphorylation status in the cytoplasm (i) or nucleus (ii) in ER+ and ER-negative cases; (iii) shows the overall distribution of pYAP(S127). (A,B) Relationships between subcellular YAP phosphorylation and nu.pERK5. (C) Relationships between YAP and nu.4ICD in ER+ and ER-negative cases. Chi-square tests were used to determine statistical significance. (D) KM analysis (with log-rank tests) of the relationships between nu.pYAP(S127), nu.4ICD and BCSS in ER+ and TNBC cases. (E) Proportions of TNBCs positive and negative for stemness and CIN markers according to nuclear YAP expression and phosphorylation. Chi-square p-value shown (*p = 0.05–0.01; **p < 0.01; p < 0.001).
BCSS, breast cancer-specific survival; CIN, chromosomal instability; CK, cytokeratin; ER, oestrogen receptor; Gem, geminin; KM, Kaplan–Meier; nu.4ICD, nuclear HER4-ICD; nu.pERK5, nuclear pERK5; TNBC, triple negative breast cancer; Vim, vimentin; YAP, yes-associated protein-1.

Shifts in YAP expression and phosphorylation during brain metastatic progression are dependent on ER status and linked to activation of HER4's tyrosine kinase activity

Next, we compared YAP expression and phosphorylation in the general breast cancer cohort, brain-metastatic breast cancers and matched brain metastases, and found significant changes across this progression series. YAP phosphorylation was significantly less frequent in brain metastatic, ER+ breast cancers than unselected ER+ cases (Figure 5A). The frequency of pYAP(S127) increased slightly in matching brain metastases, typically in both nuclei and cytoplasm, but overall the most prominent phenotype was unphosphorylated nuclear YAP (Figure 5A). Conversely, in

ER-negative disease, brain metastatic primary breast cancers had less cytoplasmic pYAP(S127), and the nuclear pYAP(S127) phenotype was unchanged. Comparison of brain metastases with matching ER-negative primary cancers indicated that YAP is more frequently expressed and phosphorylated overall (Figure 5A; top/middle panel). To account for the fact that pYAP(S127) is often present in cytoplasmic and nuclear compartments at the same time, we performed the analysis after categorising cases into subgroups with: (1) negative/low pYAP expression (light grey); (2) cytoplasm-predominant pYAP(S127) (cyto>>nucleus; orange); (3) nuclear-predominant pYAP(S127) (nucleus>>cyto; purple); or (4) high levels of pYAP(S127) in both compartments, (uniformly
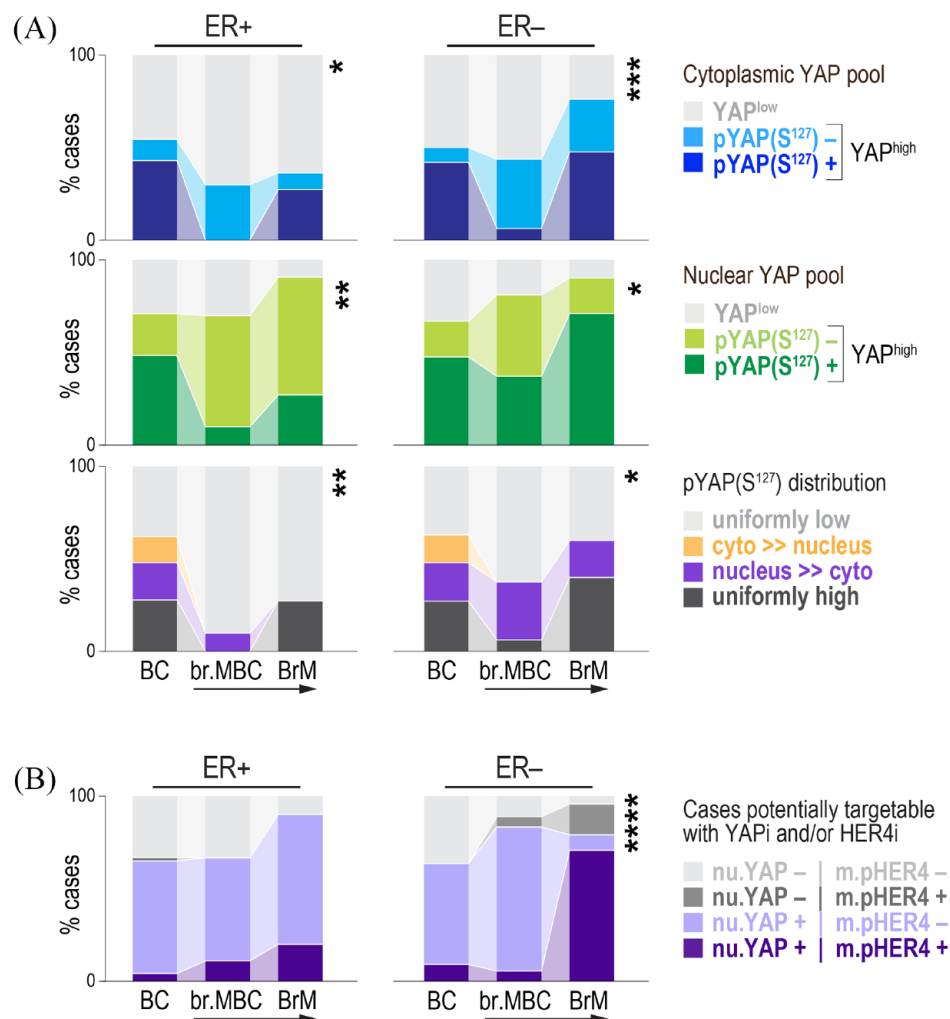
Figure 5. Expression and phosphorylation of YAP in breast cancers and matching brain metastases.
(A) Levels and phosphorylation of the cytoplasmic and nuclear YAP pools (i/ii), and pYAP(S[127]) distribution (iii) in a brain metastasis progression series comprised of the general breast cancer series (BC) plus matched br.MBC and BrM.
(B) Changes in the proportions of BC, br.MBC and BrM expressing membrane-associated pHER4 and/or nuclear YAP (phosphorylated or unphosphorylated forms). Chi-square tests used to determine statistical significance (*$p = 0.05-0.01$; **$p < 0.01$; ***$p < 0.001$; ****$p < 0.0001$).
BC, breast cancer series; BrM, brain metastases; br.MBC, brain-metastatic breast cancers; HER4, human epidermal growth factor receptor-4; YAP, yes-associated protein-1.

high; dark grey). We observed that the pYAP(S[127]) pool shifts to the nucleus during brain metastatic progression (Figure 5A).

Finally, we assessed the proportions of brain-metastatic breast cancers and matched brain metastases that could be amenable to therapeutics that target HER4's RTK activity or reduce nuclear translocation of YAP. The proportion of cases exhibiting membrane-associated pHER4 or nuclear YAP/pYAP(S[127]) was similar for ER+ and -negative breast tumours (55–60%; Figure 5B). The proportion exhibiting both phenotypes (potentially amenable to combination therapy)

was very high for ER-negative brain metastases (~70%; Figure 5B), due mostly to very frequent induction of pHER4 (Figure 2). In addition to highlighting possible therapeutic opportunities, these findings suggest that nuclear pYAP(S[127]) may be involved in transducing neuregulin signals in brain metastases, particularly those with an ER-negative phenotype.

Discussion

We previously found a high frequency of HER4 phosphorylation in brain metastases from various cancers.[16] Given that nuclear HER4-ICD activity

has been linked to YAP signalling[31,32] and YAP is an important player in metastatic breast cancer,[45] we undertook this study to investigate whether HER4 activation could be linked to YAP signalling in breast cancer brain metastases. We integrated subcellular localisation, phosphorylation and ER status in our analyses, and found that all three variables were essential to tease out specific clinicopathologic and biological correlates of HER4 and YAP, uncovering relationships that would not have been identified in analyses based on expression alone. For example, Cao and colleagues found that nuclear YAP is a favourable prognostic indicator in ER+ breast cancer,[41] while our approach clarified that the subgroup of ER+ cases with better outcome is specifically those where the nuclear YAP pool is phosphorylated.

The high frequency of nuclear pYAP(S[127]) in primary and metastatic breast tumours was somewhat surprising, since this isoform apparently represents Hippo pathway-mediated negative feedback once YAP is marked for sequestration in the cytoplasm. We found significant differences in the frequency of nuclear pYAP(S[127]) in good *versus* poor prognostic tumours, but negligible differences for cytoplasmic pYAP(S[127]). The differences were ER-dependent, with nuclear pYAP(S[127]) associated with small ER+ tumours, but larger, clinically aggressive TNBCs. These findings suggest there is major Hippo-YAP pathway dysfunction in breast cancer.

Mechanistically, it remains to be determined why pYAP(S[127]) would be present in the nucleus, but this has been observed previously.[40,45,72] It is possible that YAP is expressed at a level that overwhelms 14-3-3-mediated sequestration and/or ubiquitin-mediated proteolysis, particularly for metabolically active tumours that have a high endoplasmic reticulum stress burden.[73] Assuming that serine-127 phosphorylation marks negative feedback on YAP and that its presence in the nucleus is due to 'overflow', this implies that YAP inactivation is linked to less aggressive forms of ER+ breast cancer. TNBC aside, our findings in ER+ breast cancer (Figure 3C) are consistent with this, and with a recent report identifying YAP as a novel ERα co-factor required for oestrogen-mediated transcriptional regulation of the enhancer landscape in MCF7 cells.[74] Zhu and colleagues found that, in addition to its canonical Hippo pathway target elements, YAP co-occupies ERα-active enhancers, recruits enhancer activation machinery and may

be critical for the modulation of genome architecture by ERα.

The identification of genome-wide enhancer reprogramming as a novel mechanism of oestrogen action adds to the rationale backing efforts to develop YAP inhibitors in molecular oncology.[36] But the fact that we found high levels of nuclear pYAP(S[127]) were related to large tumour size and poor prognosis in TNBC indicates that identifying appropriate patient populations for treatment will require consideration of context-specific activity. If nuclear pYAP(S[127]) is solely the pool in excess of sequestration capabilities, these findings would suggest that YAP activity is somehow protective in ER-negative tumours, which is at odds with a body of literature suggesting otherwise,[38,75,76] and with the contrasting survival curves for cytoplasmic and nuclear pYAP(S[127]) pools in our TNBC cohort (Figure 3C). Alternative possibilities are that nuclear pYAP(S[127]) has undescribed function(s), or that Hippo pathway feedback is simply not a dominant influence on YAP activity in TNBC. Chen and colleagues mutated the equivalent phosphorylation site [YAP(S[112])] in the mouse, and found that despite major defects in cytoplasmic translocation, there were no visible developmental consequences because of a compensatory decrease in YAP protein levels.[61] The authors cautioned against extrapolating results from early mechanistic experiments (largely, *in vitro* models of contact inhibition), and against the assumption that YAP localization can be used as a surrogate for functional activity. YAP- and pYAP-specific chromatin occupancy analysis in TNBC and ER+ clinical samples should shed light on the context of its distinct functions in these settings, and ultimately help to understand why it is associated with disparate clinical outcomes.

Concerning HER4, we found that phosphorylated, membrane-associated protein is infrequent in primary breast cancers, though enriched in HER2+ cases, with Ki67 data suggesting it promotes proliferation in this context. Conversely, membrane-associated pHER4 was abundant in brain metastases. The fact that pHER4 was induced concomitantly with pHER3 indicates this is likely an adaptation to the neuregulin-rich brain microenvironment, which may lead to increased phosphorylation of YAP (Figure 5). To our knowledge, this is the first study to report these changes in a matched series of breast tumours and brain metastases. Nuclear HER4-ICD was not associated with nuclear YAP levels in any of the cohorts we analysed,

but disease-specific survival of HER4-ICD subgroups was further stratified by nuclear pYAP(S^{127}) status (Figure 4D), and the overall frequency of nuclear co-expression increased to ~50% in brain metastases (Figure 5). In principle, these findings provide support for pan-HER inhibitor clinical trials in metastatic breast cancer, with inclusion of intracranial response assessment criteria that measure clinically meaningful endpoints for patients with brain involvement.[25,77] In addition, building site-specific relapse assessment into early breast cancer trial protocols would enable assessment of any reduction in the risk of brain relapse. Combining pan-HER inhibitors with agents known to oppose YAP activity (e.g. Verteporfin, Pazopanib) would also be worthwhile exploring in a preclinical setting.

In summary, this study finds that in ER+ breast cancer, pYAP(S^{127}) is a favourable prognostic indicator. Nuclear translocation of un-phosphorylated YAP is common in brain-metastatic primary breast cancers and brain metastases with ER+ phenotypes. Conversely in ER-negative breast cancer, nuclear-localised pYAP(S^{127}) is associated with markers of aggressive clinical behaviour and relatively short survival. Nuclear pYAP(S^{127}) levels increase further when disease relapses in the brain. This co-occurs with HER4 activation in as many as 70% of ER-negative brain metastases, suggesting that combination targeting strategies could be effective.

Author contributions
Conceptualization: PK-dC, JMS; methodology/experiments: PK-dC, ML, HC, XdL, JRK, BWD, FA, PTS, AEMR; drafting, review and editing: all authors; supervision and funding: SRL, JMS; project administration: JMS.

Conflict of interest statement
The authors declare that there is no conflict of interest.

ORCID iDs
Priyakshi Kalita-de Croft [iD] https://orcid.org/0000-0001-8877-7655

Haarika Chittoory [iD] https://orcid.org/0000-0003-2793-3196

Fares Al-Ejeh [iD] https://orcid.org/0000-0002-1553-0077

Supplemental material
Supplemental material for this article is available online.

References
1. Tabouret E, Chinot O, Metellus P, *et al*. Recent trends in epidemiology of brain metastases: an overview. *Anticancer Res* 2012; 32: 4655–4662.

2. Witzel I, Oliveira-Ferrer L, Pantel K, *et al*. Breast cancer brain metastases: biology and new clinical perspectives. *Breast Cancer Res* 2016; 18: 8.

3. Posner JB and Chernik NL. Intracranial metastases from systemic cancer. *Adv Neurol* 1978; 19: 579–592.

4. Percy AK. Neoplasms of the central nervous system: epidemiologic considerations. *Neurology* 1970; 20: 398–399.

5. Tsukada Y, Fouad A, Pickren JW, *et al*. Central nervous system metastasis from breast carcinoma. Autopsy study. *Cancer* 1983; 52: 2349–2354.

6. Berghoff A, Bago-Horvath Z, De Vries C, *et al*. Brain metastases free survival differs between breast cancer subtypes. *Br J Cancer* 2012; 106: 440–446.

7. Lin NU, Amiri-Kordestani L, Palmieri D, *et al*. CNS metastases in breast cancer: old challenge, new frontiers. *Clin Cancer Res* 2013; 19: 6404–6418.

8. Hardesty DA and Nakaji P. The current and future treatment of brain metastases. *Front Surg* 2016; 3: 30.

9. Siegel RL, Miller KD and Jemal A. Cancer statistics, 2017. *CA Cancer J Clin* 2017; 67: 7–30.

10. Takei H, Rouah E and Ishida Y. Brain metastasis: clinical characteristics, pathological findings and molecular subtyping for therapeutic implications. *Brain Tumor Pathol* 2016; 33: 1–12.

11. Da Silva L, Simpson PT, Smart CE, *et al.* HER3 and downstream pathways are involved in colonization of brain metastases from breast cancer. *Breast Cancer Res* 2010; 12: R46.

12. Duchnowska R, Sperinde J, Chenna A, *et al.* Quantitative HER2 and p95HER2 levels in primary breast cancers and matched brain metastases. *Neuro Oncol* 2015; 17: 1241–1249

13. Sun M, Behrens C, Feng L, *et al.* HER family receptor abnormalities in lung cancer brain metastases and corresponding primary tumors. *Clin Cancer Res* 2009; 15: 4829–4837.

14. Woditschka S, Evans L, Duchnowska R, *et al.* DNA double-strand break repair genes and oxidative damage in brain metastasis of breast cancer. *J Natl Cancer Inst* 2014; 106.

15. Kodack DP, Askoxylakis V, Ferraro GB, *et al.* The brain microenvironment mediates resistance in luminal breast cancer to PI3K inhibition through HER3 activation. *Sci Transl Med* 2017; 9.

16. Saunus JM, Quinn MC, Patch AM, *et al.* Integrated genomic and transcriptomic analysis of human brain metastases identifies alterations of potential clinical significance. *J Pathol* 2015; 237: 363–378.

17. Law AJ, Shannon Weickert C, Hyde TM, *et al.* Neuregulin-1 (NRG-1) mRNA and protein in the adult human brain. *Neuroscience* 2004; 127: 125–136.

18. Mota JM, Collier KA, Barros Costa RL, *et al.* A comprehensive review of heregulins, HER3, and HER4 as potential therapeutic targets in cancer. *Oncotarget* 2017; 8: 89284–89306.

19. Barros FF, Powe DG, Ellis IO, *et al.* Understanding the HER family in breast cancer: interaction with ligands, dimerization and treatments. *Histopathology* 2010; 56: 560–572.

20. Kalita-de Croft P, Straube J, Lim M, *et al.* Proteomic analysis of the breast cancer brain metastasis microenvironment. *Int J Mol Sci* 2019; 20: E2524.

21. Neman J, Choy C, Kowolik CM, *et al.* Co-evolution of breast-to-brain metastasis and neural progenitor cells. *Clin Exp Metastasis* 2013; 30: 753–768.

22. Neman J, Termini J, Wilczynski S, *et al.* Human breast cancer metastases to the brain display GABAergic properties in the neural niche. *Proc Natl Acad Sci U S A* 2014; 111: 984–989.

23. Zhang L, Zhang S, Yao J, *et al.* Microenvironment-induced PTEN loss by exosomal microRNA primes brain metastasis outgrowth. *Nature* 2015; 527: 100–104.

24. Koutras AK, Fountzilas G, Kalogeras KT, *et al.* The upgraded role of HER3 and HER4 receptors in breast cancer. *Crit Rev Oncol Hematol* 2010; 74: 73–78.

25. Saura C, Oliveira M, Feng Y-H, *et al.* Neratinib + capecitabine versus lapatinib + capecitabine in patients with HER2+ metastatic breast cancer previously treated with ≥2 HER2-directed regimens: findings from the multinational, randomized, phase III NALA trial. *J Clin Oncol* 2019; 37: 1002.

26. USFDA. FDA approves neratinib for metastatic HER2-positive breast cancer. In: *Resources for Information | Approved Drugs*. USA: United States government, 2020.

27. Long W, Wagner KU, Lloyd KC, *et al.* Impaired differentiation and lactational failure of Erbb4-deficient mammary glands identify ERBB4 as an obligate mediator of STAT5. *Development* 2003; 130: 5257–5268.

28. Jones FE. HER4 intracellular domain (4ICD) activity in the developing mammary gland and breast cancer. *J Mammary Gland Biol Neoplasia* 2008; 13: 247–258.

29. Junttila TT, Sundvall M, Lundin M, *et al.* Cleavable ErbB4 isoform in estrogen receptor-regulated growth of breast cancer cells. *Cancer Res* 2005; 65: 1384–1393.

30. Wang J, Yin J, Yang Q, *et al.* Human epidermal growth factor receptor 4 (HER4) is a favorable prognostic marker of breast cancer: a systematic review and meta-analysis. *Oncotarget* 2016; 7: 76693–76703.

31. Omerovic J, Puggioni EM, Napoletano S, *et al.* Ligand-regulated association of ErbB-4 to the transcriptional co-activator YAP65 controls transcription at the nuclear level. *Exp Cell Res* 2004; 294: 469–479.

32. Haskins JW, Nguyen DX and Stern DF. Neuregulin 1-activated ERBB4 interacts with YAP to induce Hippo pathway target genes and promote cell migration. *Sci Signal* 2014; 7: ra116.

33. Hsu PC, Miao J, Huang Z, *et al.* Inhibition of yes-associated protein suppresses brain metastasis of human lung adenocarcinoma in a murine model. *J Cell Mol Med* 2018; 22: 3073–3085.

34. Shih DJH, Nayyar N, Bihun I, *et al.* Genomic characterization of human brain metastases identifies drivers of metastatic lung adenocarcinoma. *Nat Genet* 2020; 52: 371–377.

35. Dupont S, Morsut L, Aragona M, *et al.* Role of YAP/TAZ in mechanotransduction. *Nature* 2011; 474: 179–183.

36. Zanconato F, Cordenonsi M and Piccolo S. YAP and TAZ: a signalling hub of the tumour microenvironment. *Nat Rev Cancer* 2019; 19: 454–464.

37. Zhao B, Li L, Lei Q, *et al.* The Hippo-YAP pathway in organ size control and tumorigenesis: an updated version. *Genes Dev* 2010; 24: 862–874.

38. Zanconato F, Cordenonsi M and Piccolo S. YAP/TAZ at the roots of cancer. *Cancer Cell* 2016; 29: 783–803.

39. Vlug EJ, van de Ven RA, Vermeulen JF, *et al.* Nuclear localization of the transcriptional coactivator YAP is associated with invasive lobular breast cancer. *Cell Oncol* 2013; 36: 375–384.

40. Min Kim H, Kim SK, Jung WH, *et al.* Metaplastic carcinoma show different expression pattern of YAP compared to triple-negative breast cancer. *Tumour Biol* 2015; 36: 1207–1212.

41. Cao L, Sun PL, Yao M, *et al.* Expression of YES-associated protein (YAP) and its clinical significance in breast cancer tissues. *Hum Pathol* 2017; 68: 166–174.

42. Guo L, Chen Y, Luo J, *et al.* YAP1 overexpression is associated with poor prognosis of breast cancer patients and induces breast cancer cell growth by inhibiting PTEN. *FEBS Open Bio* 2019; 9: 437–445.

43. Lee JY, Chang JK, Dominguez AA, *et al.* YAP-independent mechanotransduction drives breast cancer progression. *Nat Commun* 2019; 10: 1848.

44. Yuan M, Tomlinson V, Lara R, *et al.* Yes-associated protein (YAP) functions as a tumor suppressor in breast. *Cell Death Differ* 2008; 15: 1752–1759.

45. Kim HM, Jung WH and Koo JS. Expression of Yes-associated protein (YAP) in metastatic breast cancer. *Int J Clin Exp Pathol* 2015; 8: 11248–11257.

46. Raghavendra A, Kalita-de Croft P, Vargas AC, *et al.* Expression of MAGE-A and NY-ESO-1 cancer/testis antigens is enriched in triple-negative invasive breast cancers. *Histopathology* 2018; 73: 68–80.

47. Burgess JT, Bolderson E, Saunus JM, *et al.* SASH1 mediates sensitivity of breast cancer cells to chloropyramine and is associated with prognosis in breast cancer. *Oncotarget* 2016; 7: 72807–72818.

48. Field S, Uyttenhove C, Stroobant V, *et al.* Novel highly specific anti-periostin antibodies uncover the functional importance of the fascilin 1-1 domain and highlight preferential expression of periostin in aggressive breast cancer. *Int J Cancer* 2016; 138: 1959–1970.

49. Hernandez-Perez S, Cabrera E, Salido E, *et al.* DUB3 and USP7 de-ubiquitinating enzymes control replication inhibitor Geminin: molecular characterization and associations with breast cancer. *Oncogene* 2017; 36: 4817.

50. Junankar S, Baker LA, Roden DL, *et al.* ID4 controls mammary stem cells and marks breast cancers with a stem cell-like phenotype. *Nat Commun* 2015; 6: 6548.

51. Kutasovic JR, McCart Reed AE, Males R, *et al.* Breast cancer metastasis to gynaecological organs: a clinico-pathological and molecular profiling study. *J Pathol Clin Res* 2019; 5: 25–39.

52. Wiegmans AP, Saunus JM, Ham S, *et al.* Secreted cellular prion protein binds doxorubicin and correlates with anthracycline resistance in breast cancer. *JCI Insight* 2019; 5: e124092.

53. Uhlen M, Fagerberg L, Hallstrom BM, *et al.* Proteomics. Tissue-based map of the human proteome. *Science* 2015; 347: 1260419.

54. The Cancer Genome Atlas Network. Comprehensive molecular portraits of human breast tumours. *Nature* 2012; 490: 61–70.

55. Curtis C, Shah SP, Chin S-F, *et al.* The genomic and transcriptomic architecture of 2,000 breast tumours reveals novel subgroups. *Nature* 2012; 486: 346–352.

56. Liu J, Lichtenberg T, Hoadley KA, *et al.* An integrated TCGA pan-cancer clinical data resource to drive high-quality survival outcome analytics. *Cell* 2018; 173: 400–416.e411.

57. Ni CY, Murphy MP, Golde TE, *et al.* γ-Secretase cleavage and nuclear localization of ErbB-4 receptor tyrosine kinase. *Science* 2001; 294: 2179–2181.

58. Muraoka-Cook RS, Sandahl M, Husted C, *et al.* The intracellular domain of ErbB4 induces differentiation of mammary epithelial cells. *Mol Biol Cell* 2006; 17: 4118–4129.

59. Srinivasan R, Gillett CE, Barnes DM, *et al.* Nuclear expression of the c-erbB-4/HER-4

growth factor receptor in invasive breast cancers. *Cancer Res* 2000; 60: 1483–1487.

60. Australian Institute of Health and Welfare. *Cancer in Australia 2017*. Canberra: Australian Institute of Health and Welfare.

61. Chen Q, Zhang N, Xie R, *et al*. Homeostatic control of Hippo signaling activity revealed by an endogenous activating mutation in YAP. *Genes Dev* 2015; 29: 1285–1297.

62. Lorenzetto E, Brenca M, Boeri M, *et al*. YAP1 acts as oncogenic target of 11q22 amplification in multiple cancer subtypes. *Oncotarget* 2014; 5: 2608–2621.

63. Chen TH, Chen CY, Wen HC, *et al*. YAP promotes myogenic differentiation via the MEK5-ERK5 pathway. *FASEB J* 2017; 31: 2963–2972.

64. Huang J, Wu S, Barrera J, *et al*. The Hippo signaling pathway coordinately regulates cell proliferation and apoptosis by inactivating Yorkie, the Drosophila Homolog of YAP. *Cell* 2005; 122: 421–434.

65. Hao Y, Chun A, Cheung K, *et al*. Tumor suppressor LATS1 is a negative regulator of oncogene YAP. *J Biol Chem* 2008; 283: 5496–5509.

66. Komuro A, Nagai M, Navin NE, *et al*. WW domain-containing protein YAP associates with ErbB-4 and acts as a co-transcriptional activator for the carboxyl-terminal fragment of ErbB-4 that translocates to the nucleus. *J Biol Chem* 2003; 278: 33334–33341.

67. Cordenonsi M, Zanconato F, Azzolin L, *et al*. The Hippo transducer TAZ confers cancer stem cell-related traits on breast cancer cells. *Cell* 2011; 147: 759–772.

68. Wang L, Zhang Z, Yu X, *et al*. Unbalanced YAP-SOX9 circuit drives stemness and malignant progression in esophageal squamous cell carcinoma. *Oncogene* 2019; 38: 2042–2055.

69. Overholtzer M, Zhang J, Smolen GA, *et al*. Transforming properties of YAP, a candidate oncogene on the chromosome 11q22 amplicon. *PNAS* 2006; 103: 12405–12410.

70. Al-Ejeh F, Simpson PT, Saunus JM, *et al*. Meta-analysis of the global gene expression profile of triple-negative breast cancer identifies genes for the prognostication and treatment of aggressive breast cancer. *Oncogenesis* 2014; 3: e124.

71. Abdel-Fatah TMA, Ball GR, Thangavelu PU, *et al*. Association of sperm associated antigen 5 and treatment response in patients with estrogen receptor positive breast cancer. *JAMA Network Open* 2020; 3: e209486.

72. Cho YS, Zhu J, Li S, *et al*. Regulation of Yki/Yap subcellular localization and Hpo signaling by a nuclear kinase PRP4K. *Nat Commun* 2018; 9: 1657.

73. Adwal A, Kalita-de Croft P, Shakya R, *et al*. Tradeoff between metabolic i-proteasome addiction and immune evasion in triple-negative breast cancer. *Life Sci Alliance* 2020; 3.

74. Zhu C, Li L, Zhang Z, *et al*. A Non-canonical role of YAP/TEAD is required for activation of estrogen-regulated enhancers in breast cancer. *Mol Cell* 2019; 75: 791–806.e798.

75. Andrade D, Mehta M, Griffith J, *et al*. YAP1 inhibition radiosensitizes triple negative breast cancer cells by targeting the DNA damage response and cell survival pathways. *Oncotarget* 2017; 8: 98495–98508.

76. Li Y, Wang S, Wei X, *et al*. Role of inhibitor of yes-associated protein 1 in triple-negative breast cancer with taxol-based chemoresistance. *Cancer Sci* 2019; 110: 561–567.

77. Alexander BM, Brown PD, Ahluwalia MS, *et al*. Clinical trial design for local therapies for brain metastases: a guideline by the Response Assessment in Neuro-Oncology Brain Metastases working group. *Lancet Oncol* 2018; 19: e33–e42.

Visit SAGE journals online
journals.sagepub.com/home/tam

SAGE journals